Photonic gaps in the dispersion of surface plasmons on gratings

W. L. Barnes, T. W. Preist, S. C. Kitson, J. R. Sambles, N. P. K. Cotter, and D. J. Nash
Department of Physics, Exeter University, Exeter, Devon, EX4 4QL, United Kingdom
(Received 8 November 1994)

An analytic model is presented that reveals the physical origin of the photonic band gap created by Bragg scattering of surface plasmon polaritons on gratings. The model leads to simple functional forms for the gap width, central frequency, and field distributions which are confirmed by comparison with numerical calculations and experimental data.

The propagation of waves through periodic media is fundamental to the understanding of many physical phenomena, for example, the electrical conduction of crystals. There is currently great interest in the interaction of light with media that are periodic at optical wavelengths.[1-3] In a way similar to the conduction of electrons through a crystal, energy gaps open up in the dispersion relation for the propagation of light through such media when the wavelength of the light is commensurate with the periodicity of the material, creating a photonic band gap. Interest in such phenomena is intense because it offers the possibility of controlling the optical properties of materials, particularly spontaneous emission, by design at the mesoscopic scale (10–1000 nm).[3] We report in this paper on band gaps that arise for the propagation of surface plasmon polaritons on a corrugated metallic surface. Such band gaps have been reported before[4-8] and have been used to control phenomena such as surface enhanced Raman scattering.[7] We present in this Brief Report a theoretical description that provides a clear physical explanation for the origin of the band gap and the associated field distributions. In addition, direct comparison between our analytic theory, a full numerical solution to the problem, and experimental data provide confirmation of the theoretical model.

Surface plasmon polaritons (SPP's) are electromagnetic modes which may propagate along the interface between two media whose optical permittivities are of opposite sign. We consider the situation of SPP's propagating on a metallic grating, with their wave vector perpendicular to the grating grooves. If the wave vector of the SPP mode is κ and that of the grating is 2κ, then Bragg scattering of the mode occurs and a SPP standing wave will be set up. Using symmetry arguments we expect two standing wave solutions; one with field maxima at the grating peaks, the other with maxima at the grating troughs. Since there is an energy associated with the SPP field distribution we expect the two standing-wave solutions to have different energies; this will manifest itself as a gap in the dispersion curve of the SPP. Consequently we have formulated a model that concentrates on the surface modes rather than the overall optical response of the system, as has been done by previous authors.[9-14] In so doing we provide simple analytic expressions for both the gap width and the central frequency. Further, we confirm our expectation from symmetry arguments as to the location of the standing-wave solutions, and find that the energy difference arises from the way in which the electromagnetic fields and associated surface charges are distributed with respect to the grating.

The defining solution of the electromagnetic field equations for a SPP mode propagating on a planar interface separating two regions of relative permittivity ε_1 and ε_2 arises from the matching of the tangential E and H field components. This leads to the condition $k_z^{(1)}/\varepsilon_1 = k_z^{(2)}/\varepsilon_2$ where $k_z^{(1)}$ and $k_z^{(2)}$ are the components of the mode wave vector normal to the surface. Consider a SPP with wave vector κ and angular frequency ω. This mode has associated fields that decrease exponentially away from the interface in both regions, that is, $k_z^{(1)} = i\eta_1$ and $k_z^{(2)} = -i\eta_2$, so that

$$\frac{\eta_1}{\varepsilon_1} + \frac{\eta_2}{\varepsilon_2} = 0 \tag{1}$$

with $\eta_i = [\kappa^2 - (\omega/c)^2 \varepsilon_i]^{1/2}$. From Eq. (1) we see that the surface mode exists if ε_1 and ε_2 have real parts of opposite sign, when the above condition implies that $(\omega_0/c)^2 = \kappa^2(1/\varepsilon_1 + 1/\varepsilon_2)$, the dispersion relation for a SPP on a planar interface.

Consider the corresponding situation when the surface has a nonplanar profile that has periodic components in the form

$$f(x) = a \sin(\kappa x) + b \sin(2\kappa x) .$$

The periodicity of 2κ associated with the b term couples left and right moving surface modes of wave vector κ, while the periodicity of κ associated with the a term couples normal incidence external radiation to the modes. If a is small then the dominant coupling between the $\pm\kappa$ SPP modes, or more generally between symmetric and antisymmetry combinations of these, comes from the b term. In the absence of the grating these combinations represent two degenerate solutions of frequency ω_0, but when the grating is present the degeneracy is removed, and the new solutions are appropriate linear combinations of the symmetric and antisymmetric standing waves. Experimentally it is well established that an energy gap opens up,[4-8] and we wish to determine its magnitude and the central frequency of this gap. Since Eq. (1) was obtained by matching the field distributions at the planar surface we must now analogously match the fields

0163-1829/95/51(16)/11164(4)/$06.00

across the corrugated surface.

A variety of methods have been used in numerical computation to satisfy the boundary conditions on the corrugated surface, but a method developed by Chandezon *et al.*[15] is particularly appropriate. The application of this method to the current problem involves the following stages.

(1) The transformation of Maxwell's equations to a nonorthogonal coordinate system $v=x$, $w=y$, and $u=z-f(x)$ since in these coordinates the surface is described by $u=$const.

(2) For propagation normal to the grooves there is no dependence on y (or w) and any solution to Maxwell's equations in each region can be developed in the form $F(u,v)=\sum_q F_q(u,v)$, where

$$F_q(u,v)=\begin{bmatrix} H_q(u,v) \\ E_q(u,v) \end{bmatrix}=\exp(i\lambda^q u)\sum_m \begin{bmatrix} f_m^q \\ g_m^q \end{bmatrix}\exp(im\kappa v) .$$

$F_q(u,v)$ is an eigensolution associated with propagation in the "u direction" involving the eigenvalue λ_q (the analog of k_z in the planar case) and $\psi^q=\binom{f^q}{g^q}$ is the associated eigenvector that determines the relative magnitude of the Fourier components of the tangential E and H fields in the solution. We are concerned with only the surface plasmon (TM) modes so that the associated E field will lie in the xz plane and the H field will be in the y direction.

(3) The model developed assumes that the dominant mechanism responsible for the gap is the coupling of the degenerate symmetric and antisymmetric standing modes of wave vector κ via the 2κ component of the grating. Within this model it is further assumed that $\kappa b \ll 1$, and that terms of order $(kb)^4$ and higher are negligible.

Solutions on either side of the interface are expressed as linear combinations of the symmetric and antisymmetric standing mode eigenvectors ψ_+ and ψ_-. Matching of the associated tangential fields at the boundary yields the following coupled equations that replace Eq. (1):

$$\begin{aligned} \frac{1}{\varepsilon_1}[i\eta_1+\xi+\mu(i\eta_1-\xi)]&=\frac{1}{\varepsilon_2}[-i\eta_2+\xi+\mu(-i\eta_2-\xi)] , \\ \frac{1}{\varepsilon_1}[i\eta_1-\xi+\mu(-i\eta_1-\xi)]&=\frac{1}{\varepsilon_2}[-i\eta_2-\xi+\mu(i\eta_2-\xi)] , \end{aligned} \tag{2}$$

where $\xi=\kappa^2 b(1-\frac{3}{2}\rho)$ and $\eta_i(\omega)=[\kappa^2(1-\rho)^2+\xi^2-\varepsilon_i(\omega/c)^2(1-\rho)]^{1/2}$, with $\rho=2(\kappa b)^2$; μ is the ratio of the amplitudes of ψ_- and ψ_+. Equation (2) implies that $\mu=\mp i$ with corresponding frequencies $\omega_\pm$. Strictly speaking one should include the dependence of ε_i upon ω as considered by Seshadri[12–14] but in the context of the small frequency shifts considered here this effect is negligible.

The solution of Eqs. (2) for $\omega_\pm$ yields the following exact results (within the framework of the model):

$$\frac{\Delta\omega^2}{c^2}=\left[\frac{\omega_+}{c}\right]^2-\left[\frac{\omega_-}{c}\right]^2=\frac{4\kappa^2(\kappa b)}{\sqrt{-\varepsilon_1\varepsilon_2}}[1-3(\kappa b)^2] , \tag{3a}$$

$$\frac{\overline{\omega^2}}{c^2}=\frac{1}{2}\left[\left[\frac{\omega_+}{c}\right]^2+\left[\frac{\omega_-}{c}\right]^2\right]=\left[\frac{\omega_0}{c}\right]^2[1-2(\kappa b)^2] \tag{3b}$$

and

$$\eta_1(\omega_\pm)=\eta_1^0(1-\rho)\mp\xi , \tag{4a}$$

$$\eta_2(\omega_\pm)=\eta_2^0(1-\rho)\pm\xi , \tag{4b}$$

where $\eta_1^0=\kappa(-\varepsilon_1/\varepsilon_2)^{1/2}$ and $\eta_2^0=\kappa(-\varepsilon_2/\varepsilon_1)^{1/2}$ are the inverse decay lengths for a planar surface. Note that for an ideal metal $\varepsilon_2\to-\infty$ and there is no gap.

Before examining these results let us look at what our model tells us about the field distributions for the two standing-wave solutions. There are three field components associated with the modes, $H_\parallel^\pm$, $E_\parallel^\pm$, and $E_N^\pm$, where $\parallel$ and N refer to parallel and normal to the local surface. From the model we find that at the grating surface $H_\parallel^\pm, E_\parallel^\pm \propto \cos(\kappa v\mp\pi/4)$, and that $E_N^\pm, \sigma^\pm \propto \sin(\kappa v\mp\pi/4)$, where $\sigma^\pm$ is the surface charge density associated with the mode. Thus in the high-frequency solution the normal field component and charge distribution have a maximum amplitude at the troughs of the 2κ component whereas for the low-frequency solution they occur at the peaks.

The decay of the fields away from the interface are determined by $\eta_1(\omega_\pm)$ and $\eta_2(\omega_\pm)$. Typically medium 1 is a dielectric and medium 2 a metal, for which $\varepsilon_2<0$. From Eqs. (4) we see that $\eta_1(\omega_+)<\eta_1^0$, $\eta_2(\omega_+)>\eta_2^0$, whereas $\eta_1(\omega_-)>\eta_1^0$, $\eta_2(\omega_-)<\eta_2^0$ so that for the high-frequency solution the field is enhanced in the dielectric and reduced in the metal; the converse is true for the low-frequency solution. The grating perturbs the field distributions associated with the charges. When the charges are located at the troughs the field is squeezed in the dielectric and extended in the metal resulting in an increase in energy, the opposite is true when the charges are located at the peaks, see Fig. 1. It is now clear that the energy difference arises from the different configurations that the electromagnetic field and associated charges take with respect to the grating for the two solutions. This is confirmed by an explicit calculation of the total energy associated with the field and surface charge distributions derived from the model presented above.

In addition we are able to compare the results of our model with those obtained using a full numerical solution to the problem—one that combines the approach of Chandezon *et al.*[15] mentioned above with a scattering matrix formalism.[16] In Fig. 1 we show the result of calculating the normal electric field distribution E_N close to the grating surface for the high- and low-frequency solutions. The results confirm the nature of the mode solutions discussed above for both the position of the field maxima and the decay length of the two solutions.

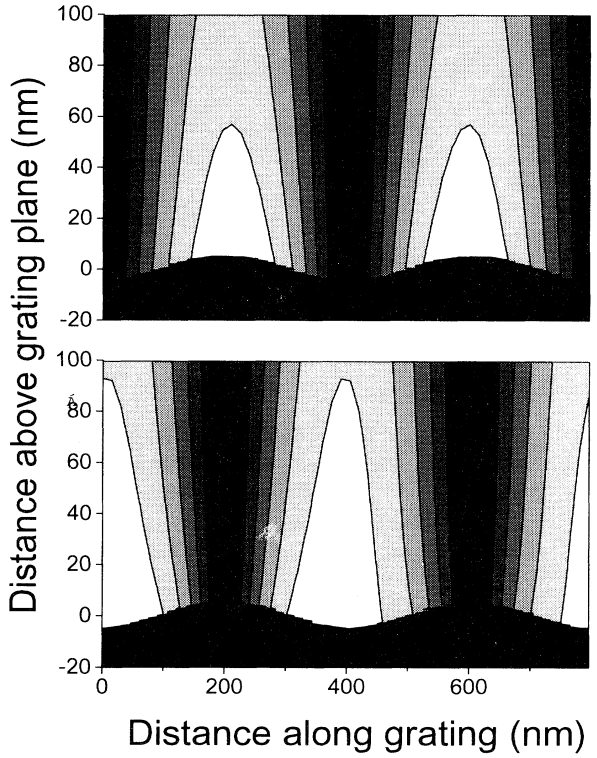

FIG. 1. The spatial distribution of the normal electric field component, $|E_N|$, for the low energy (top diagram) and high energy (bottom diagram) standing wave SPP mode solutions. Regions of high field strength are shown white. For these data the ratio of the amplitudes of the fundamental to harmonic components have been set to $a/b=0.04$; the profile seen is thus that of the 2κ grating.

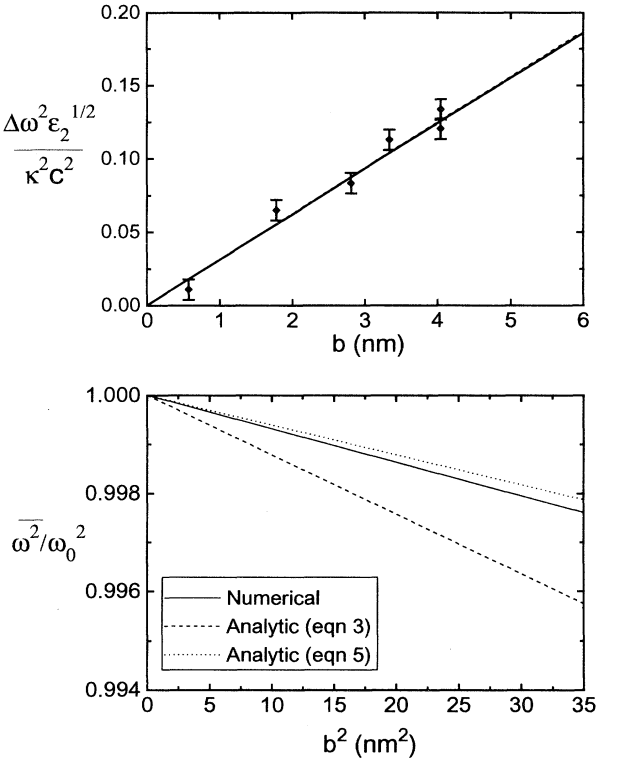

FIG. 2. The gap width [defined and normalized in an appropriate way, see Eqs. (3a) and (5a)] as a function of the amplitude b of the 2κ periodic component (top diagram) and $\overline{\omega^2}$ as a function b^2. The results of calculations from both Eqs. (3) and (5) of our model are presented together with those of the full numerical simulation. Experimental results are also included for the gap. Note that the data from the numerical calculations and that of Eq. (5) for the gap overlap.

We can also compare the functional forms of our model, Eq. (3), with those obtained numerically. To do this we find the reflectivity minima associated with the SPPs and monitor their frequency as we change b. The result of doing this, and a comparison with our simple model, is shown in Fig. 2. We see that, as expected from the model presented here, Eq. (3), $\Delta\omega^2$ is linearly proportional to b. We also see that $\overline{\omega^2}$ falls as b increases. This latter behavior is in agreement with that predicted numerically by Glass and Maradudin[10] but is in marked contrast to that of Seshadri[12] who predicted that the central frequency would rise with increasing b. However, the model outlined above predicts, in Eq. (3), a fall in $\overline{\omega^2}$ that is considerably larger than that found from the full numerical calculation, see Fig. 2. The origin of this discrepancy is that the 2κ component of the grating also provides coupling between the κ and 3κ SPP modes and coupling between the $-\kappa$ and -3κ modes. This coupling introduces additional terms of order $(\kappa b)^2$ not included in the above model. Extending the model to evaluate the correction terms changes Eq. (3) to

$$\frac{\Delta\omega^2}{c^2}=\left[\frac{\omega_+}{c}\right]^2-\left[\frac{\omega_-}{c}\right]^2=\frac{4\kappa^2(\kappa b)}{\sqrt{-\varepsilon_1\varepsilon_2}}\left[1-\tfrac{7}{2}(\kappa b)^2\right], \tag{5a}$$

$$\frac{\overline{\omega^2}}{c^2}=\frac{1}{2}\left[\left[\frac{\omega_+}{c}\right]^2+\left[\frac{\omega_-}{c}\right]^2\right]=\left[\frac{\omega_0}{c}\right]^2\left[1-(\kappa b)^2\right]. \tag{5b}$$

This latter form for $\overline{\omega^2}$ gives much better agreement with the numerical calculations. Although the change in the expression for $\Delta\omega^2$ is small, it too provides better agreement; these improvements are shown in Fig. 2.

We note that we solved our analytic model assuming the metal to be lossless. Figure 2 compares experimental data with that of both the numerical model, in which the dielectric constant for the gold is taken as $-25+2.5i$, and the analytic model. The good agreement between the three validates the lossless assumption in the analytic model in calculating the position and width of the gap. If instead we are concerned with the gap's effectiveness, i.e., how much of the incident energy is reflected rather than coupled to the system, then loss in the metal becomes important. The width of the surface plasmon resonances is increased by such loss so that if the magnitude of the gap is small the modes may overlap and incident light will be

partially absorbed rather than totally reflected. However, the reflectivity in the gap also depends on the relative coupling strengths of the two modes, which in turn depends on the relative phase of the κ and 2κ components, the effect of which is the subject of ongoing work.

Let us now return to our results for the energy gap. As discussed above Eq. (5) shows to first order that the width of the gap is linear in b, as found by others using optical response theories.[9,14] Previously these results were checked against experimental work undertaken by Pockrand and analyzed by Raether,[17] producing an apparent discrepancy. However, in that experimental work a "momentum gap" rather than an "energy gap" was measured. The experiment involved examining the dispersion curve by scanning the momentum for a range of fixed frequencies, achieved by measuring the reflectivity as a function of angle of incidence. More recently Weber and Mills[18] have shown how such experiments can give rise to misleading results for the energy gap and showed that the reflectivity should be measured by scanning the frequency with the momentum (angle of incidence) held fixed. Since these previous results are inappropriate we undertook a frequency scanning experiment to determine the functional dependence of the gap width on the amplitude b of the 2κ component of the grating.

In our experiments gold gratings were produced by coating corrugated silica substrates. By examining the frequency dependence of the reflectivity of these samples as a function of angle of incidence, the band gap is readily determined.[8] The gratings have twice the pitch needed to produce the requisite wave vector for a band gap at the desired frequency. Nonlinearities in the holographic fabrication of the grating meant that they had two main periodic components: one at the fundamental pitch having a wave vector of κ which serves to couple the surface modes to photons, a second with half this pitch and thus wave vector, 2κ: it is this latter component that provides the Bragg scattering to form the energy gap. The amplitude of the Fourier components of the gratings at κ and 2κ were determined by fitting theoretical models to the angular dependence of the reflectivity of the bare gold gratings. Our experimental results for $\Delta\omega^2$ as a function of the amplitude b are shown in Fig. 2, confirming the linearity to within experimental error. We further find them to be in excellent agreement with the results of both our model presented here, and the full numerical solution. Our experimental data are unable to confirm or deny the change in $\overline{\omega^2}$ with b as given by Eq. (5b) because the grating amplitudes are too small and because of the contribution from other terms in the surface profile, particularly the κ component.

In conclusion we have presented a new analytic model that provides a physical explanation for the origin of the photonic band gap due to Bragg scattering of surface plasmon polaritons on gratings. The details of the model have been compared to both numerical and experimental data with good agreement. The model provides an easy way to predict the width and position of energy gaps with experimentally relevant parameters. Work is currently in progress to confirm experimentally the shift in $\overline{\omega^2}$ with the amplitude b, to examine large amplitude gratings, and to extend the study to crossed gratings.

The authors wish to acknowledge the financial support of the Engineering and Physical Sciences Research Council and the Defence Research Agency (Malvern).

[1]E. Yablonavitch, Phys. Rev. Lett. **58**, 2059 (1987).
[2]S. John, Phys. Rev. Lett. **58**, 2486 (1987).
[3]E. Yablonavitch, J. Opt. Soc. Am. **10**, 283 (1993).
[4]R. H. Ritchie, E.T. Arakawa, and R. H. Hamm, Phys. Rev. Lett. **21**, 1530 (1968).
[5]Y. J. Chen, E. S. Koteles, R. J. Seymor, G. J. Sonek, and J. M. Ballantyne, Solid State Commun. **46**, 95 (1983).
[6]D. Heitmann, N. Kroo, C. Schulz, and Zs. Szentirmay, Phys. Rev. B **35**, 2660 (1987).
[7]W. Knoll, M. R. Philpott, J. D. Swalen, and A. Girlando, J. Chem. Phys. **77**, 2254 (1982).
[8]D. J. Nash, N. P. K. Cotter, E. L. Wood, G. W. Bradberry, and J. R. Sambles, J. Mod. Opt. **42**, 243 (1995).
[9]D. L. Mills, Phys. Rev. B **15**, 3097 (1977).
[10]N. E. Glass and A. A. Maradudin, Phys. Rev. B **24**, 595 (1981).
[11]E. Popov, Surf. Sci. **222**, 517 (1989).
[12]S. R. Seshadri, J. Appl. Phys. **57**, 4874 (1985).
[13]S. R. Seshadri, J. Appl. Phys. **57**, 5098 (1985).
[14]S. R. Seshadri, J. Appl. Phys. **58**, 1733 (1985).
[15]J. Chandezon, M. T. Dupuis, G. Cornet, and D. Maystre, J. Opt. Soc. Am. **72**, 839 (1982).
[16]N. P. K. Cotter, T. W. Preist, and J.R. Sambles, J. Opt. Soc. Am. A (to be published).
[17]*Surface Polaritons,* edited by V. M. Agranovitch and D. L. Mills (North-Holland, Amsterdam, 1982), p. 393.
[18]M. G. Weber and D. L. Mills, Phys. Rev. B **34**, 2893 (1986).

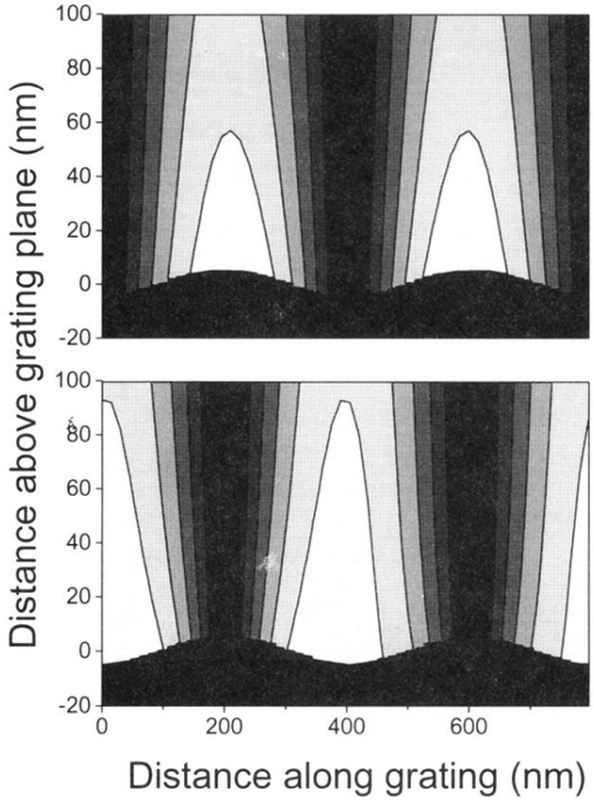

FIG. 1. The spatial distribution of the normal electric field component, $|E_N|$, for the low energy (top diagram) and high energy (bottom diagram) standing wave SPP mode solutions. Regions of high field strength are shown white. For these data the ratio of the amplitudes of the fundamental to harmonic components have been set to $a/b = 0.04$; the profile seen is thus that of the 2κ grating.